On Membrane Motor Activity and Chloride Flux in the Outer Hair Cell: Lessons Learned from the Environmental Toxin Tributyltin

Lei Song,*‡ Achim Seeger,‡ and Joseph Santos-Sacchi*†‡
Otolaryngology,* Neurobiology,† and Surgery,‡ Yale University School of Medicine, New Haven, Connecticut

ABSTRACT The outer hair cell (OHC) underlies mammalian cochlea amplification, and its lateral membrane motor, prestin, which drives the cell's mechanical activity, is modulated by intracellular chloride ions. We have previously described a native nonselective conductance (G_{metL}) that influences OHC motor activity via Cl flux across the lateral membrane. Here we further investigate this conductance and use the environmental toxin tributyltin (TBT) to better understand Cl-prestin interactions. Capitalizing on measures of prestin-derived nonlinear capacitance to gauge Cl flux across the lateral membrane, we show that the Cl ionophore TBT, which affects neither the motor nor G_{metL} directly, is capable of augmenting the native flux of Cl in OHCs. These observations were confirmed using the chloride-sensitive dye MQAE. Furthermore, the compound's potent ability, at nanomolar concentrations, to equilibrate intra- and extracellular Cl concentrations is shown to surpass the effectiveness of G_{metL} in promoting Cl flux, and secure a quantitative analysis of Cl-prestin interactions in intact OHCs. Using malate as an anion replacement, we quantify chloride effects on the nonlinear charge density and operating voltage range of prestin. Our data additionally suggest that ototoxic effects of organotins can derive from their disruption of OHC Cl homeostasis, ultimately interfering with anionic modulation of the mammalian cochlear amplifier. Notably, this observation identifies a new environmental threat for marine mammals by TBT, which is known to accumulate in the food chain.

INTRODUCTION

Sensitive hearing in mammals relies on cochlear amplification, and is thought to result from the voltage-dependent motor activity of outer hair cells (OHCs) (Brownell et al., 1985; Ashmore, 1987; Santos-Sacchi and Dilger, 1988). The motor protein prestin, which resides exclusively in the lateral membrane (Belyantseva et al., 2000), is likely key to this process (Zheng et al., 2000; Liberman et al., 2002). Recent studies suggest that prestin activity is highly dependent on the intracellular chloride (Cl) anion. Oliver et al. (2001) found that removing intracellular Cl abolishes the motor's nonlinear charge movement (or nonlinear capacitance, NLC), thereby blocking OHC motility. However, the story is actually more complicated than initially thought, since we discovered that some effects of Cl removal result from induced shifts in prestin's operating voltage range, and not from elimination of motor charge movement (Rybalchenko and Santos-Sacchi, 2003a,c; Santos-Sacchi, 2003). Indeed, substitution of intracellular Cl with other anions, such as sulfonate derivatives or malate, results in a shift of motor function along the voltage axis, the direction of which depends on the substituted anion (Rybalchenko and Santos-Sacchi, 2003b,c): the voltage at peak NLC (V_{pkcm}) ranges from −180 mV for pentane-sulfonate substitution to +100 mV for malate substitution. Since Cl is the physiologically abundant intracellular anion, it probably sets the operating position of NLC and motor function in the OHC. This operating position hovers around the physiological resting potential, namely ~−70 mV (Dallos et al., 1982).

Considering the importance of Cl ions in OHC function, regulation of Cl transport across the lateral membrane is paramount. Little is known about processes that control chloride flux in OHCs (Gitter et al., 1986; Kawasaki et al., 1999; Rybalchenko and Santos-Sacchi, 2003a,c), though we have identified an unusual stretch-sensitive conductance localized to the lateral membrane, G_{metL}, that passes chloride and consequently can modulate prestin activity. A more detailed understanding of chloride's role in intact OHCs is needed, and could help in understanding normal as well as pathological cochlear function.

The organotin compounds trimethyl (TMT) and triethyl (TET) tin are known to cause auditory dysfunction, which has been attributed to disrupted calcium homeostasis (Clerici et al., 1991; Fechter et al., 1986, 1992; Liu and Fechter, 1995). Indeed, the effects of organotins on other physiological processes also have been linked to their untoward influence on Ca mechanisms (Kishimoto et al., 2001). Interestingly, though, organotin compounds can act as Cl ionophores (Tosteson and Wieth, 1979; Wieth and Tosteson, 1979), with tributyltin (TBT) being three orders of magnitude more effective than TMT at promoting anion exchange diffusion. The halides and hydroxyl anions can participate in heteroexchange with Cl across the membranes of red cells and mitochondria, as well as artificial bilayers (Motais et al., 1977; Selwyn et al., 1970; Wieth and Tosteson, 1979; Tosteson and Wieth, 1979). Intrinsic chloride conductance of the membrane is unaffected, and at concentrations below a few micromolar the intrinsic membrane dipole is unperturbed

Submitted September 27, 2004, and accepted for publication November 29, 2004.

Address reprint requests to Joseph Santos-Sacchi, Sections of Otolaryngology and Neurobiology, Yale University School of Medicine, BML 246, 333 Cedar St., New Haven, CT 06510. Tel.: 203-785-5407; Fax: 203-737-2502; E-mail: joseph.santos-sacchi@yale.edu.

0006-3495/05/03/2350/13 $2.00

doi: 10.1529/biophysj.104.053579

(Tosteson and Wieth, 1979). Because TBT readily promotes Cl flux, it is routinely used to equilibrate intracellular and extracellular Cl to calibrate chloride-sensitive fluorescent dyes, such as MQAE (*N*-(ethoxycarbonylmethyl)-6-methoxyquinolinium bromide) (Verkman, 1990; Marandi et al., 2002). Among the organotins, TBT in particular is an internationally recognized environmental threat to marine life since it accumulates in the food chain, and remains a commonly used antifouling compound for large boat bottoms (U.S. Environmental Protection Agency, 2004).

Here we study the effects of TBT on Cl exchange across the OHC lateral membrane to gain insight into the function of the anion's natural pathway, G_{metL}, and assure ourselves of uncompromised control of Cl on both sides of the OHC's lateral membrane. We find rapid and profound effects of TBT on OHC NLC, which are directly related to the toxin's ability to transport Cl across the OHC membrane. Consequently, we have been able to obtain definitive and quantitative information on Cl-prestin interactions in native, intact OHCs. We also conclude that organotin ototoxicity ultimately results from interference with the anionic control of mammalian cochlear amplification, and, accordingly, we identify the marine mammal's auditory periphery as an especially susceptible target for the pervasive environmental toxin TBT.

MATERIALS AND METHODS

Hartley albino guinea pigs were overdosed with halothane. Temporal bones were excised and the organ of Corti was exposed under a dissection microscope in calcium-free extracellular medium. The top three turns of the organ of Corti were dissected from the cochlea, and the dissected segments were digested with dispase I (0.5 mg/ml) in a nominally (no chelator) calcium free extracellular medium for 10–12 min. After resuspension in 1 mM chloride extracellular medium (see below), cells were isolated by gentle trituration. The solution was then placed in a plastic petri dish to allow OHCs to settle. A Nikon Eclipse E600-FN microscope with Hoffmann optics was used to observe cells during the electrical measurements.

The base extracellular solution contained NaCl (140 mM), $CaSO_4$ (2 mM), $MgSO_4$ (1.2 mM), and Hepes (10 mM). The intracellular solution contained NaCl (140 mM), $CaSO_4$ (2 mM), $MgSO_4$ (1.2 mM), Hepes (10 mM), and EGTA (10 mM). Cl concentrations were 0.1, 0.2, 0.5, 1, 5, 10, 20, 40, 80, 140, and 200 mM. Cl concentration was adjusted by substituting Cl with the divalent anion malate. In a subset of experiments, gluconate was the major substitute. Final solutions were adjusted to ~300 mOsm (except for the solutions that contain 200 mM Cl) with dextrose and adjusted to pH 7.2~7.3 with NaOH. A stock solution of TBT (200 mM) was made in ethyl alcohol (EtOH) and then diluted in extracellular medium to obtain the desired concentrations. To dissociate the effect of TBT from EtOH, in a subset of experiments, TBT was directly mixed with extracellular medium to obtain desired concentrations (under the assumption that TBT totally dissolves in the alcohol-free solution). In these control experiments, the actual concentration of TBT is undetermined but likely to be lower than those equivalent solutions prepared using EtOH stock solution.

A custom-made Y-tube perfusion system was used for the delivery of experimental solutions to individual OHCs during continuous chamber wash with control extracellular solution. Perfusions were made with a range of chloride concentrations in combination with varying TBT levels. For the first set of experiments, we used either 5 or 140 mM Cl extracellular solution with varying TBT concentrations (0.01, 0.1, 1, 10, and 50 μM). In the next set of experiments, TBT concentrations were fixed at 1 μM, but Cl concentrations were varied (1, 5, 10, 20, 40, 80, 140, and 200 mM). NLC was permitted to reach steady state before any subsequent manipulation. Perfusion speed through the Y-tube was 20 μl/min with the tip placed 150–200 μm away from the patched cells. In this setup, junction potentials (calculated with Jpcalc; Axon Instruments, Union City, CA) associated with malate are small, and not corrected [<9 mV absolute for the largest changes from 1-mM to 140-mM Cl solutions, assuming a mobility for malate of 0.4 relative to Cl; direct measures of junction potentials were much smaller (2–3 mV)]. For the quantitative analysis of chloride level effects on motor activity, solutions were matched intracellularly and extracellularly (except that intracellular solutions had an additional 10 mM EGTA; see above), thus avoiding junctional potential effects.

Single OHCs were studied under whole-cell voltage clamp. An Axon 200B amplifier was used to hold the cell at 0 mV to remove the electrical drive for Cl ion flux. Thus, the effects of our imposed Cl concentration gradients were studied in isolation. Initial pipette resistances were 4–7 MΩ. Series resistances, which ranged from 5 to 20 MΩ, remained uncompensated for C_m measurements. Before establishing whole-cell configuration, gigohm seals were obtained (1.5–3.5 GΩ), and stray pipette capacitance was neutralized. All data acquisition and analysis was performed with a Windows-based patch-clamp program jClamp (www.SciSoftCo.com). Voltage was corrected offline for the effects of series resistance.

NLC was calculated using a continuous high-resolution (2.56-ms sampling) two-sine stimulus protocol (10 mV peak at both 390.6 and 781.2 Hz) superimposed onto a voltage ramp (200-ms duration) from either −200 to +80 mV or −160 to +120 mV (Santos-Sacchi et al., 1998b). Capacitance data were fit to the first derivative of a two-state Boltzmann function (Santos-Sacchi, 1991),

$$C_m = Q_{max}\frac{ze}{kT}\frac{b}{(1+b)^2} + C_{lin}, \quad (1)$$

where

$$b = \exp\left(\frac{-ze(V_m - V_{pkCm})}{kT}\right),$$

Q_{max} is the maximum nonlinear charge moved, V_{pkcm} is voltage at peak capacitance or, equivalently, at half maximum charge transfer, V_m is membrane potential, z is valence, C_{lin} is linear membrane capacitance, e is electron charge, k is Boltzmann's constant, and T is absolute temperature.

Q_{sp} (specific nonlinear charge) was calculated as $Q_{max}/(C_{lin} - 6.5)$, where C_{lin} is the linear capacitance, a measure of surface area, obtained from Boltzmann fits (Santos-Sacchi and Navarette, 2002). A value of 6.5 pF in linear capacitance is the estimated contribution of apical and basal ends of the OHC, and therefore is subtracted to provide only that lateral membrane area that contains prestin (Huang and Santos-Sacchi, 1993; Santos-Sacchi, 2004). To determine unbiased estimates of linear capacitance we employed the following logic and strategy. The capacitance of the OHC is an asymmetric bell-shaped function due to motor surface area change; on average the left side of the function asymptotes at a value 3.5 pF greater than the right asymptote (Santos-Sacchi and Navarrete, 2002). C_{lin} is defined as the minimum capacitance, that is, when all the motors are in the compact state (right side of function). However, since the NLC curve shifts depending on intracellular Cl concentration and substitute anion, in some cases C_{lin} was not directly measurable because the right side was truncated. To assure accurate estimates of C_{lin} across cells with different intracellular Cl concentrations, all cells were first fitted only to the left half of the NLC curve to obtain an initial estimate of Q_{max} and z. Q_{max} and z were then used to estimate motor number ($N = Q_{max}/ze$), and the offset capacitance proportional to motor surface area change was determined from Fig. 4 *c* in Santos-Sacchi and Navarrete (2002). By subtracting this offset from the left-side asymptote of the NLC function we obtained an unbiased estimate of C_{lin}. It should be noted, however, that all final estimates of Q_{max} and z reported in this manuscript were determined from fits of Eq. 1 to full NLC datasets. All curve fitting was performed offline with jClamp and derived

parameters were analyzed in Excel and Sigma Plot (Jandel Scientific, San Rafael, CA). Plots were generated by using Sigma Plot. Standard errors are reported.

Chloride flux experiments were performed using fluorescence imaging of OHCs loaded with the Cl-sensitive dye MQAE, obtained from Molecular Probes (Eugene, OR). Isolated OHCs incubated in 1 mM Cl extracellular solution were placed onto coverslips coated with Cell-Tak (BD Biosciences, San Jose, CA). Cells were then moved to a thermostatically controlled microperfusion chamber, and incubated with 10 mM MQAE dye in the dark for 30 min. After excess dye was flushed off the coverslips, cells were examined under an inverted microscope with 60× magnification (IX70, Olympus, Tokyo, Japan) and images were captured through a Photometrics (Tucson, AZ) cooled CCD camera and analyzed with the program Metafluor (Universal Imaging, Downingtown, PA). The bath solutions were then changed in the following order: 1 mM Cl, 145 mM Cl, 1 mM Cl with 10 μM TBT, 145 mM Cl with 10 μM TBT and 145 mM Cl. The solution exchange rate was 4 ml/min by gravity flow into a 0.6-ml chamber. Measurements were carried out with excitation at 350 ± 10 nm and emission at 450 ± 10 nm. For presentation, noncellular background fluorescence, measured simultaneously, was subtracted from cellular responses. Photobleaching of the dye was insignificant on the timescale of our measurements; this is indicated by the return of fluorescence to the same 1 mM Cl pretreatment level after exposure to 145 mM Cl (see Fig. 1).

RESULTS

TBT promotes chloride flux across the OHC membrane

It is firmly established that TBT promotes Cl exchange across membranes (Motais et al., 1977; Selwyn et al., 1970; Wieth and Tosteson, 1979; Tosteson and Wieth, 1979; Verkman, 1990). However, to confirm that TBT also enhances Cl flux in OHCs, experiments were carried out with the use of the Cl-sensitive fluorescent dye MQAE. In MQAE-loaded isolated OHCs that were preincubated in 1 mM chloride extracellular solution, a switch to 145 mM extracellular chloride solution caused a quenching of the dye's fluorescence, indicating that an increased chloride gradient resulted in an influx of chloride via the OHC's native conductance G_{metL} (Fig. 1). The addition of TBT markedly enhanced the influx of chloride. Thus, the OHC membrane is no different in its susceptibility to TBT than the other membranes previously studied.

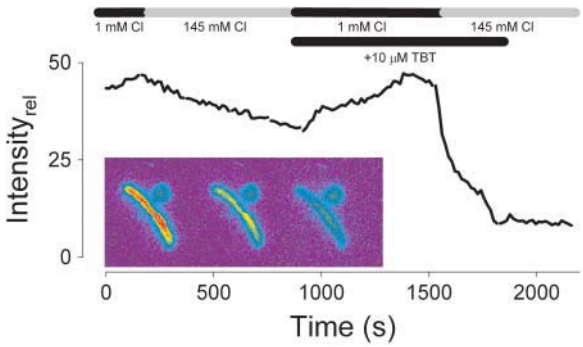

FIGURE 1 TBT promotes enhanced Cl flux across the OHC lateral membrane as measured by the fluorescent, chloride-sensitive dye MQAE. A dye-loaded OHC was perfused with the following solutions (indicated by the *bars* in the figure): 1 mM Cl, 145 mM Cl, 1 mM Cl with 10 μM TBT, 145 mM Cl with 10 μM TBT, and 145 mM Cl. Emission light intensity drops when the intracellular dye is quenched due to an increase in intracellular chloride. The chloride flux during the initial chloride gradient step, i.e., through G_{metL}, is less than that during a subsequent gradient step in the presence of TBT. Time resolution was 7.5 s. (*Inset*) Another example of an OHC showing fluorescence image changes. Cell width is 10 μm. At zero time (*left panel*), the OHC bath was switched from 1 mM to 140 mM Cl extracellular solution. (*Middle panel*) At 360 s after, and (*right panel*) 945 s after switch. Flux is through G_{metL} alone, since TBT is absent in this case. The quenching of fluorescence (red → green) indicates an increase in intracellular Cl.

TBT affects NLC only in the presence of a chloride gradient across the OHC

To further study the effect of TBT on OHC chloride flux during perfusion of TBT, we monitored NLC, which we and others have shown to be a very sensitive indicator of intracellular chloride levels (Oliver et al., 2001; Rybalchenko and Santos-Sacchi, 2003c). In the steady-state presence of a chemical gradient of Cl across the OHC lateral membrane (140 mM outside, 5 mM inside), and in the absence of TBT, V_{pkcm} is stable near −10 mV (Fig. 2 *A*, *rightmost trace*). This stability under these recording conditions arises from a net balance of Cl movements via G_{metL} and the patch pipette, resulting in a stable Cl activity at the intracellular aspect of prestin. However, in the presence of extracellular TBT, V_{pkcm} shifts leftward (hyperpolarizing direction) and the absolute magnitude of the shift increased with increasing TBT concentration (Fig. 2, *A* and *C*, *solid symbols*). This incrementing shift arises from the enhanced Cl exchange, which more effectively counters pipette washout, since, as we show below, TBT has no effect on prestin itself. At high levels (>10 μM), TBT caused membrane instability and loss of recordings; we therefore limited most of our work to a 1-μM concentration.

It is conceivable that TBT may directly interfere with Cl-prestin interactions, thereby contributing to the observed results. To rule out this possibility, we compared the effects of TBT on NLC in the absence of a driving force for Cl transport (5 mM inside, 5 mM outside; Fig. 2 *B*). In the absence of a gradient, there cannot be a diffusion-based net movement of Cl. However, if TBT were to alter the interaction between Cl and prestin, there would be a dose-dependent effect of TBT upon NLC measures. We chose to use 5 mM intrapipette Cl to ensure that prestin works in the midrange of its dose-response curve (Oliver et al., 2001), allowing alterations in prestin activity to be easily discerned. Under these conditions, perfusion of TBT at varying concentrations did not induce significant shifts of V_{pkcm} or changes in peak capacitance (Fig. 2, *B* and *C*, *open symbols*).

TBT does not directly affect prestin or G_{metL}

Since chloride affects the state probability of prestin (Rybalchenko and Santos-Sacchi, 2003c), it is possible that a chloride gradient can set prestin into a permissive state

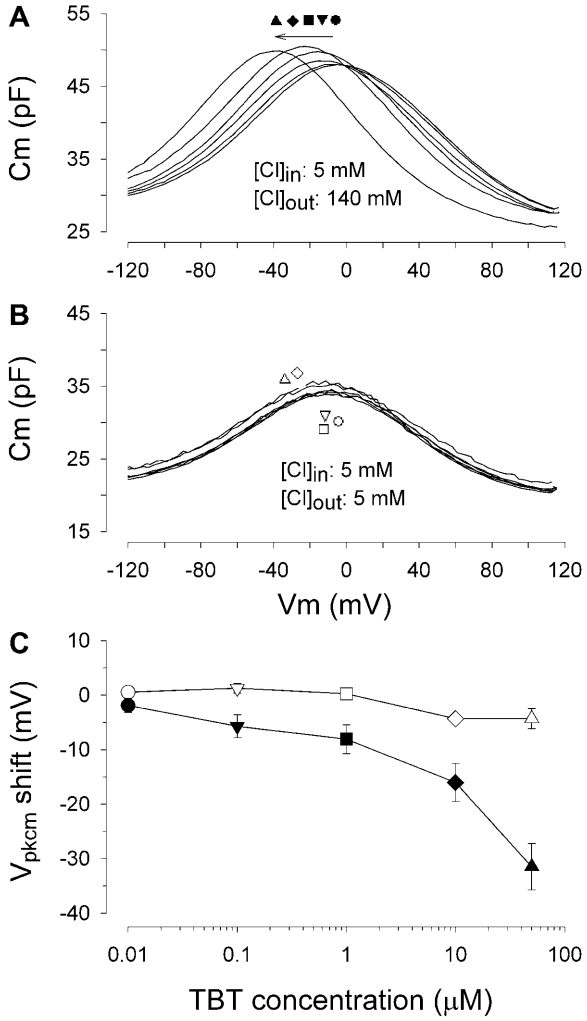

FIGURE 2 Effects of TBT upon V_{pkcm} depend on the chloride concentration gradient across the OHC membrane. (*A*) A representative cell with the pipette solution containing 5 mM Cl and the extracellular solution containing 140 mM Cl. The NLC curve shifts left with increasing extracellular TBT concentration (from right to left: 0 (*rightmost trace*), 0.01 (*solid circle*), 0.10 (*solid upside-down triangle*), 1.0 (*solid square*), 10 (*solid diamond*), and 50 (*solid triangle*) μM), as the Cl exchange more effectively counters pipette washout. (*B*) A representative cell with both the pipette and extracellular solution containing 5 mM Cl. Regardless of TBT concentration, the NLC remains virtually unchanged. (*C*) Average responses of two groups as in *A* and *B* ($n = 5$–8); each cell in a group was exposed to the full concentration range. Open and solid symbols represent cells bathed in the extracellular media containing 5 and 140 mM Cl, respectively. Gluconate was used to substitute for Cl in bath solution. Symbol types correspond to different TBT concentrations (as used in *A*, above). TBT effects were statistically significant (paired *t*-test; $p < 0.05$) for all concentrations except 10 nM.

whereby TBT could directly act on the protein, in analogy to well known state-dependent effects of blockers on ion channels. To evaluate this possibility, we directly probed the state dependence of TBT effects on prestin by driving the motor into predominantly the expanded or compact state with voltage (−50 and + 50 mV; no chloride gradient, 140 mM in/out), while noting the effects of TBT on NLC (Fig. 3). The overlapping NLC traces at either holding voltage in the presence or absence of TBT indicates that any state dependence of direct TBT effects on the motor is absent. The difference in the traces obtained at either holding voltage is due to the effect of prior voltage on NLC that we thoroughly described previously (Santos-Sacchi et al., 1998b). In a similar fashion, we also tested nonsaturating chloride conditions (5 mM in, 140 mM out) to determine whether chloride interactions with prestin might be modified by TBT. The basic results were the same—there was no differential action on motor activity by TBT at either holding potential. These data confirm that TBT does not directly affect prestin or its interaction with chloride.

Another possibility that could account for shifts in V_{pkcm} is a direct action of TBT on G_{metL}, which naturally would only be effective in the presence of a Cl gradient. To rule out this possibility, we measured OHC membrane conductance directly during treatments with TBT in the presence of a Cl

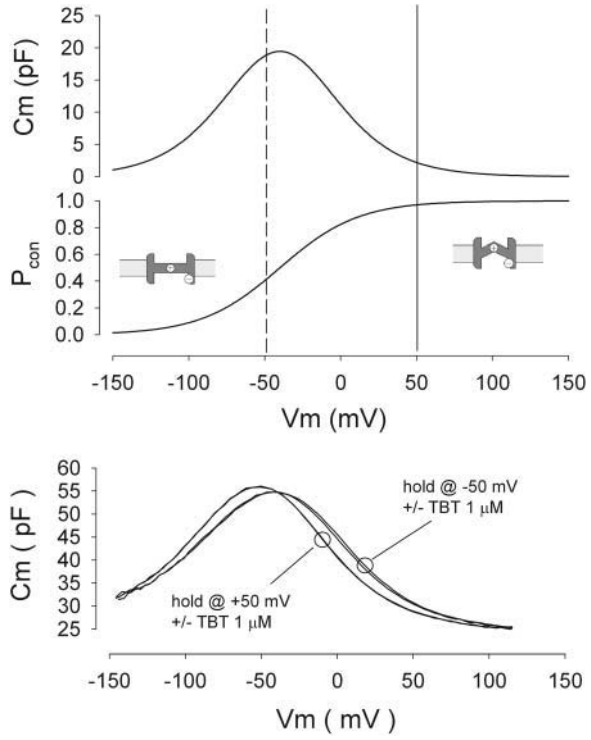

FIGURE 3 TBT does not work on the motor directly in a state-dependent manner. The top two panels indicate the relationship between NLC and motor-state probability, or population distribution of the motors into either the compact or expanded state. Hyperpolarization increases the number of motors in the expanded state. At the two vertical lines the number of motors in each state markedly differs. The lower panel shows four NLC traces. The overlapping traces obtained at +50 mV with and without 1 mM TBT test to see if TBT works selectively on the motors when predominantly in the expanded state; those traces obtained under the same conditions except at −50 mV test the effects of TBT when most motors are in the compact state. No Cl gradient is present (140 mM in/out). The overlap of the traces at either holding voltage indicates a lack of a state-dependent effect of TBT directly on the motors. The difference between the traces at each holding potential is fully a result of prior voltage effects on NLC (Santos-Sacchi et al., 1998b).

gradient (5 mM in/ 140 mM out). Fig. 4, *A* and *B*, shows that membrane resistance actually increases slightly, i.e., G_{metL}, which we measure directly, decreases during perfusions with TBT, whereas NLC shows typical effects of Cl modulation (Fig. 4 *C*). Under our ionic recording conditions (see Methods) G_{metL} is mainly responsible for setting R_m. Additionally, the inset of Fig. 4 *A* shows the percent change in membrane resistance caused by 1 μM TBT in the absence of a chloride gradient for different Cl concentrations. TBT decreases conductance by a few percent. These data indicate that TBT does not induce Cl movements by activating G_{metL} or any another conductance.

The effects of TBT on NLC depends on the magnitude and direction of the chloride gradient

Taken together our data thus far, namely, the direct measure of chloride flux with MQAE, the absence of direct effects of TBT on prestin and G_{metL}, and the requirement for a chloride gradient, strongly indicate that TBT works simply by augmenting the flux of Cl into and out of the OHC in a manner that we have previously shown to occur via G_{metL} (Rybalchenko and Santos-Sacchi, 2003c). The following observations, which show directional and magnitude sensitivity of the chloride gradient on NLC, confirm this conclusion and support the similar conclusions of others (Tosteson and Wieth, 1979; Wieth and Tosteson, 1979; Marandi et al., 2002).

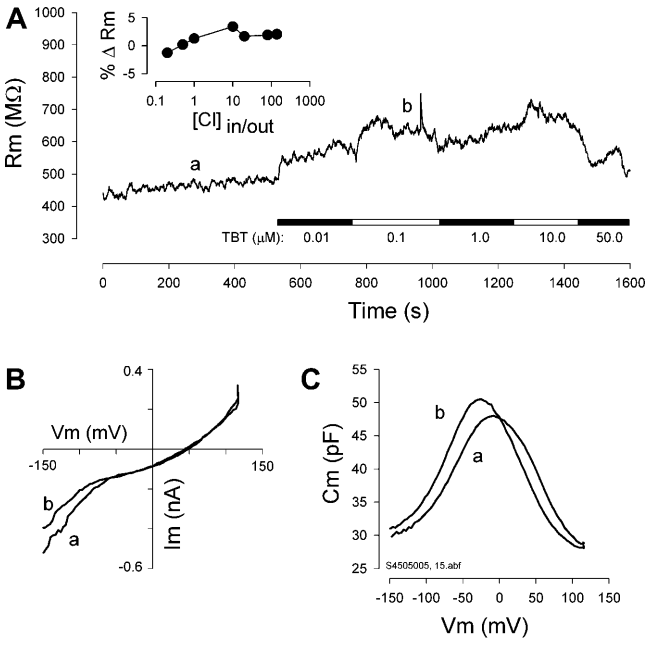

FIGURE 4 TBT does not activate the native Cl pathway, G_{metL}. (*A*) Continuous measures of R_m (determined with 10 mV step hyperpolarizations at 0 mV holding potential) were made during local perfusion of an OHC with different TBT concentrations with a chloride gradient similar to what we expect in vivo, namely, 140 mM outside/5 mM inside. (*Inset*) The plot shows the percent change in membrane resistance caused by 1 μM TBT in the absence of a chloride gradient for different Cl concentrations. TBT decreases conductance by a few percent. (*B*) *i-v* curves from positions *a* and *b* marked in *A*. Slope resistance of each curve (*a* and *b*) at 0 mV differs by ~30% as indicated in *A*. (*C*) NLC obtained simultaneously at *a* and *b*. During the first 8–9 min, in the absence of TBT, the NLC stabilized, as depicted in *C* (*trace a*). Upon addition of TBT, membrane conductance actually decreased and is indicated by the *i-v* curve in *B*, indicating a reduction of Cl movements through G_{metL}; however, despite the reduction of Cl movement via membrane conductance, the increase in intracellular Cl via anion exchange diffusion via TBT causes a negative shift in NLC (*C*, *trace b*). Similar results were obtained in eight cells. These data indicate that TBT does not work by nonselectively increasing membrane conductance or by increasing G_{metL}.

OHCs bathed in 1 mM Cl medium for extended periods of time (up to 2 h) retain a significant concentration of Cl intracellularly, based on initial whole-cell measures of NLC (Fig. 5). The retention of higher chloride levels is likely because the cells are collapsed under this condition, and the stretch-activated G_{metL} is not fully activated. Immediately after establishing whole-cell configuration, V_{pkcm} hovered around −40 mV (Fig. 5 *A*, *leftmost NLC curve*). At the start of cytoplasmic washout with pipette solutions containing 1 mM Cl, recordings made every 25 s revealed that V_{pkcm} shifted to the right as intracellular Cl levels dropped. Accompanying the shift was a reduction of Q_{max}. Eventually steady-state conditions were reached, indicated by the accumulation of overlapping NLC curves (Fig. 5 *A*). The time course of the pipette washout process was exponential, with time constants of 80.44 ± 7.3 s for V_{pkcm} and 44.87 ± 5.5 s for Q_{max} (mean ± SE; paired *t*-test, $p = 0.004$; Fig. 5, *B* and *C*), the difference in time constants possibly indicating independence of the underlying mechanisms responsible for each of the parameters. However, changes in the Boltzmann fit during the shift, resulting from truncations of tail regions of the NLC function due to voltage limitations, conceivably could contribute to this difference. Steady-state levels were reached in 3–5 min, as expected for washout through patch pipettes (Pusch and Neher, 1988); the reason for this stabilization may be that the intracellular Cl concentration finally matched the extracellular concentration or, as noted above, that a stable Cl activity at the intracellular aspect of prestin was achieved. These possibilities are evaluated below.

Since it appears that the impact of TBT on prestin derives from its ionophore effect (Figs. 2–4), a change in the driving force for Cl, namely a change in the mismatch between intra- and extracellular Cl concentrations, should substantially modulate prestin activity, just as occurs with the native conductance G_{metL} (Rybalchenko and Santos-Sacchi, 2003c). To evaluate this possibility, we studied the consequences of changes in extracellular Cl levels with or without the addition of TBT. After steady-state intracellular washout with 1-mM Cl solutions (as in Fig. 6), perfusion of extracellular solutions with graded Cl concentrations (5–140 mM in the absence of TBT) shifted NLC functions back to the left, with a slight change in Q_{max} (Fig. 6, *A*, *C*, and *E*). However, even with the highest Cl concentration extracellularly, V_{pkcm} did not shift more than −20 mV. Furthermore, above 80 mM extracellular Cl, effects seem to saturate (Fig. 6, *A* and *C*),

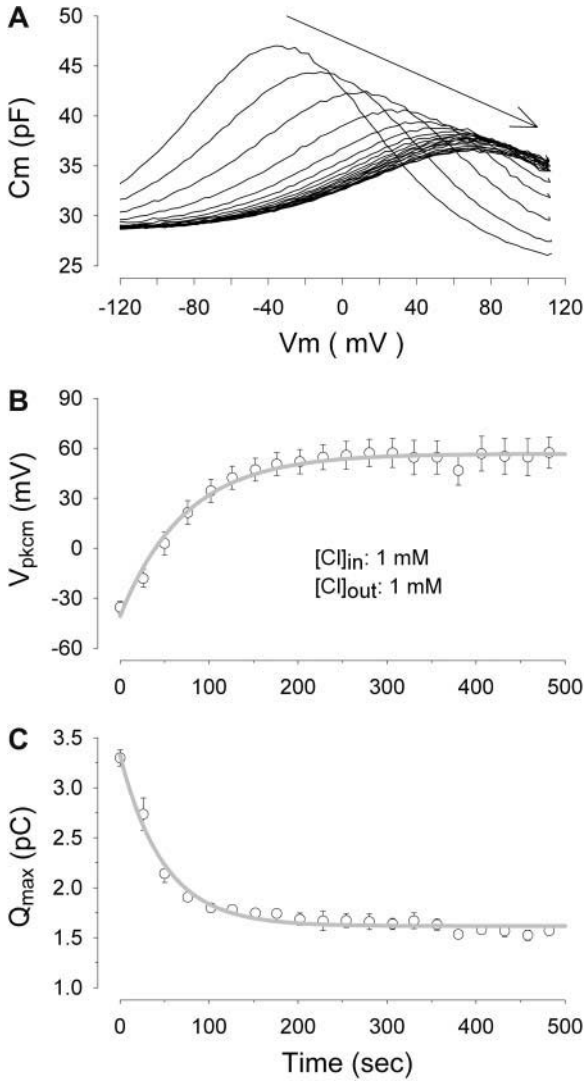

FIGURE 5 Effects of intracellular chloride washout on NLC. Cells were bathed in 1 mM Cl extracellular solutions for up to 2 h to reach steady state. The initial recordings were obtained within 5–10 s after establishment of whole-cell configuration with pipette solutions containing 1 mM Cl. (*A*) A representative cell with an initial V_{pkcm} near −40 mV. Recordings were made every 25 s until steady state was reached. The NLC curve shifted quickly to the right with the reduction of magnitude. At steady state, NLC curves overlapped. (*B* and *C*) Averaged V_{pkcm} and Q_{max} derived from four cells with complete data sets. The thick lines are fits to averaged data and averaged time constants are 80.44 ± 7.3 s for V_{pkcm}, and 44.87 ± 5.5 s for Q_{max}.

indicating the limited capability of the native Cl conductance, G_{metL}, to overcome the continuous pipette-mediated cell washout of Cl (i.e., given a finite G_{metL} (Rybalchenko and Santos-Sacchi, 2003c)).

As we anticipated, the addition of TBT in the perfusion medium augments Cl influx, which is clearly indicated by measures of prestin activity (Fig. 6 *B*). Shown in Fig. 6 *B* are the responses from the same cell depicted in Fig. 6 *A* but now reperfused (after a steady-state return to 1 mM Cl extracellular solutions) with identical Cl concentration steps containing 1 μM TBT. In the presence of TBT, V_{pkcm} continuously shifted leftward and Q_{max} increased as extracellular Cl concentration was increased (Fig. 6, *B*, *D*, and *F*). In fact, the initial V_{pkcm} (*dashed line*, similar to leftmost curve in Fig. 5 *A* but showing a more positive potential due to the delayed start of the initial recording) was recovered when extracellular Cl reached 140 mM, which corresponds to a >-50 mV shift. When the extracellular Cl concentration was increased further to 200 mM (~380 mOsm, an unnatural osmolarity and Cl concentration), an additional V_{pkcm} shift of −13 mV was observed (Fig. 6 *B*, *leftmost curve*). These data clearly show that TBT provides an additional route for Cl influx, whose efficiency, unlike that of the cell's natural Cl conductance, G_{metL}, can more effectively counter the continuous consequences of pipette washout. During the resultant changes in intracellular chloride levels, OHC shape is expected to change as V_{pkcm} shifts; for example, at a fixed holding voltage, a hyperpolarizing shift in V_{pkcm} will be sensed as a depolarizing stimulus by the voltage sensors of the lateral membrane motors. This we observed as a contraction of OHCs when local extracellular Cl perfusion was switched from 1 mM to 80 mM in the presence of TBT, as illustrated in Fig. 7. The magnitude of this contraction indicates that in addition to a voltage-induced contraction, water influx additionally shortens the cell (see Discussion).

We were able to use TBT to study Cl efflux as well as influx, since the compound works by diffusional exchange (Tosteson and Wieth, 1979; Wieth and Tosteson, 1979). In this case, we observed recovery from extracellular perfusions of high Cl concentrations in the presence and absence of TBT (Fig. 8). Initially, cells were patched with 1 mM Cl intra- and extracellularly, and NLC was allowed to reach steady-state conditions, as in Fig. 5. Then cells were loaded with Cl by perfusing with high extracellular Cl in the absence of TBT (either 80 or 140 mM), and allowed to reach steady state again. Upon returning to 1-mM Cl extracellular solutions in the absence of TBT, V_{pkcm} and Q_{max} recovered only partially toward the initial low Cl, control condition (Fig. 8). The subsequent addition of 1 μM TBT into the extracellular solution quickly completed the recovery toward the control condition (Fig. 8). The inability of G_{metL} to foster a recovery to the same conditions as it permitted before loading may indicate that the conductance is rectified. Alternatively, the conductance may have changed during the intervening time during perfusions (see Discussion).

The chloride-Q_{max} and chloride-V_{pkcm} dose-response function in the intact OHC

NLC in OHCs is clearly influenced by intracellular Cl concentration, and its magnitude and voltage dependence are determined by prestin's Cl dose-response function (Oliver et al., 2001; Rybalchenko and Santos-Sacchi, 2003c). When pipette solutions contain 20 mM Cl, perfusions of higher

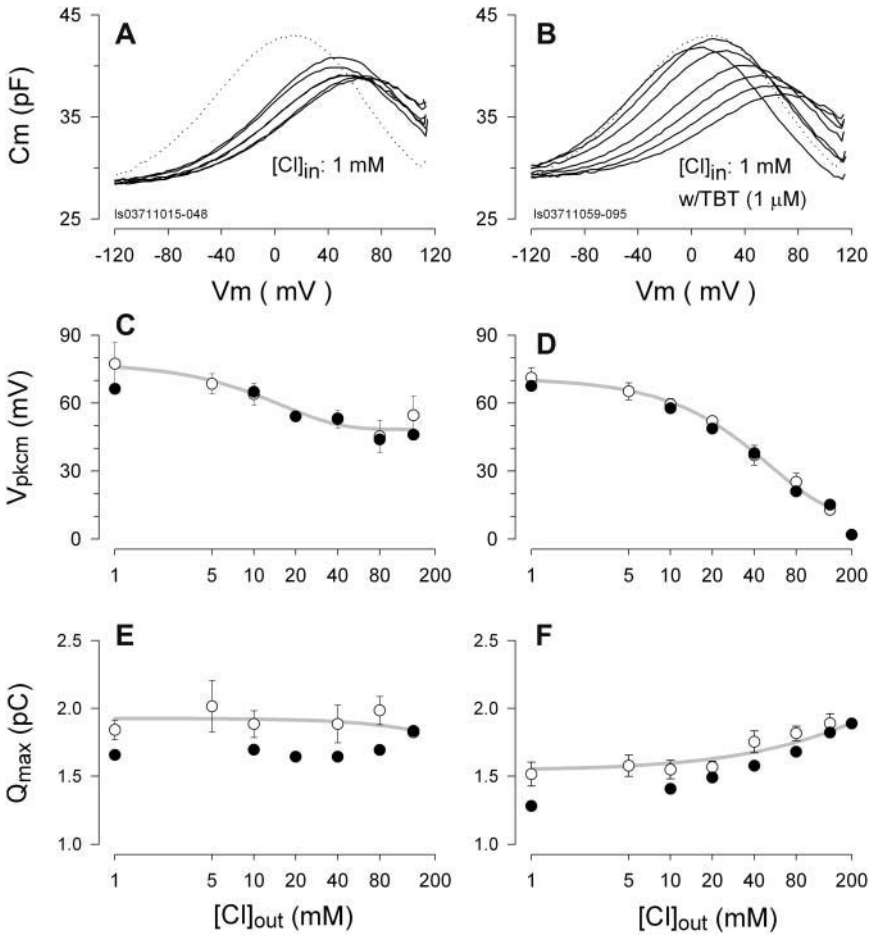

FIGURE 6 Reperfusion of high chloride extracellular solutions recovers prestin activity. (*A* and *B*) Response from the same representative cell. With the reperfusion of high Cl extracellular solution, either in the presence or absence of TBT, NLC shifts back toward the original condition (i.e., the first NLC trace measured upon whole-cell pop-in, plotted as *dashed line*, similar to leftmost trace in Fig. 5 *A*). However, in the absence of TBT, G_{metL} is unable to provide a sufficiently rapid Cl influx to overcome the effects of continuous pipette washout of Cl; the shift of V_{pkcm} did not recover beyond +40 mV (*A*). With the addition of TBT (1 μM; *B*), NLC shifts back to the control level. Derived V_{pkcm} and Q_{max} are plotted in panels (*C–F*) Solid circles represent the results from the sample cell. Open circles are averages ± SE.

concentrations of extracellular Cl, with or without TBT, do not significantly shift NLC functions (data not shown), suggesting that Cl - prestin interactions are nearly saturated at this concentration. Oliver et al. (2001) found a $K_{1/2}$ for intracellular Cl of 6.3 mM based on Q_{max} estimates in membrane patches. We measured the NLC functions of intact OHCs under symmetrical intracellular and extracellular Cl concentrations of 0.2, 0.5, 1, 5, 10, 20, 80, and 140 mM. To ensure symmetrical conditions, TBT was used in a subset of experiments, but no statistically significant differences were noted. For example, comparing TBT versus no TBT at 1 mM Cl, Q_{max} was 1.64 ± 0.07 vs. 1.69 ± 0.04 pC (mean ± SE; $n = 12$, $n = 27$; $p = 0.53$); similarly, for V_{pkcm}, 73.34 ± 4.99 vs. 63.96 ± 3.55 mV ($n = 12$, $n = 27$; $p = 0.14$). As another example, at 80 mM Cl comparisons showed 3.17 ± 0.22 vs. 3.20 ± 0.14 pC ($n = 5$, $n = 10$; $p = 0.94$) and −54.63 ± 6.85 vs. −52.38 ± 5.47 mV ($n = 5$, $n = 10$; $p = 0.80$), respectively. This absence of effects is in line with the data from Fig. 2, and confirmed that the intracellular and extracellular concentrations of Cl were truly equilibrated. Thus, data were pooled, and using a logistic fit, our estimated $K_{1/2}$ for Q_{sp} (Santos-Sacchi et al., 1998a) is 6.06 ± 2.34 mM and slope is 1.02 ± 0.5 (Fig. 9 *A*); a similar fit was made to the V_{pkcm} data giving 4.48 ± 0.77 and 0.94 ± 0.17, respectively (Fig. 9 *B*). A significant proportion of motor charge was insensitive to Cl. That is, ~36% of the nonlinear charge movement remained intact in the absence of Cl. It is important to note that the anion used to replace Cl influences V_{pkcm} and Q_{max} (Rybalchenko and Santos-Sacchi, 2003c), and that the insensitive proportion of motor charge can be much larger for other anion substitutes. For example, intracellular washout with malate substitution at 5 mM Cl stabilizes at a Q_{sp} of 0.13 ± 0.005 pC ($n = 19$), whereas substitution with gluconate provides a Q_{sp} of 0.18 ± 0.006 pC ($n = 17$). This difference corresponds to an equivalent shift along the concentration axis of ~+9 mM Cl for malate-based solutions. In other words, the Q_{sp} value with 5 mM Cl in gluconate-based solutions equals the Q_{sp} value measured from 16 mM Cl in malate-based solutions.

The ethanol vehicle for TBT delivery does not influence NLC

In the preparation of TBT stock solution, ethyl alcohol (EtOH) was used to dissolve TBT that otherwise would have been incompletely dissolved in water-based solutions. To evaluate the impact of EtOH, in a subset of experiments, OHCs were perfused with graded concentrations of EtOH

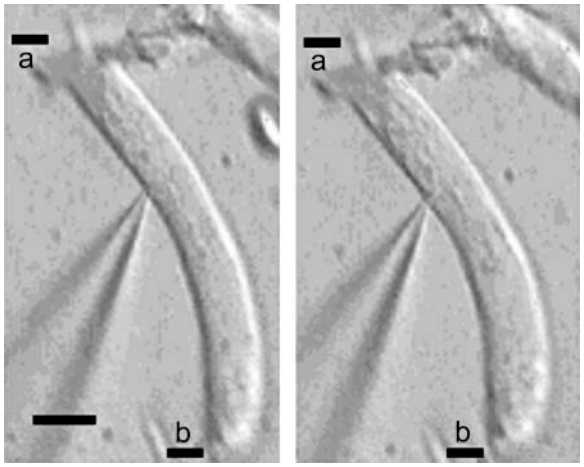

FIGURE 7 Influx of Cl causes OHC contraction. A representative OHC was locally perfused with extracellular medium that contained 1 mM (*left*) and 80 mM (*right*) Cl. TBT (1 μM) is present in both cases. The fiducial mark is the pipette tip, which remains fixed. Pipette solution contained 1 mM Cl. Small debris are inescapably disturbed by the constant flow. Scale bar (*bottom left*) is 10 μm. *a*, line at cell apex; *b*, line at cell base.

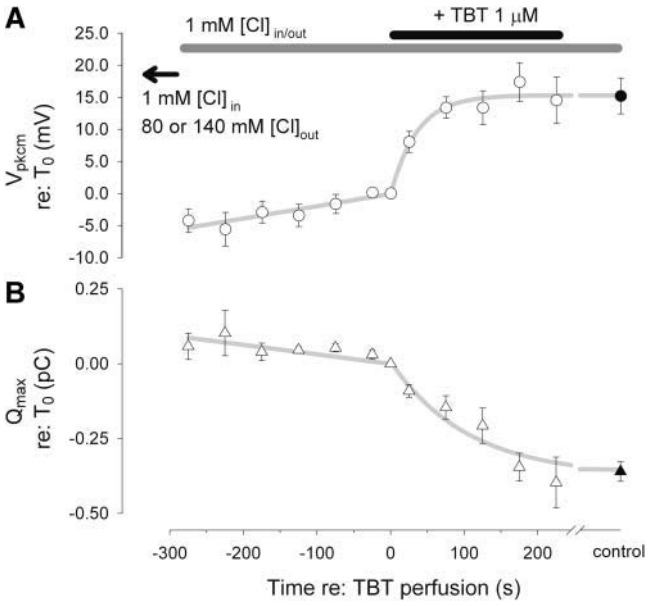

FIGURE 8 TBT enhances Cl efflux. (*A* and *B*) Aaverages ($n = 7$) of relative V_{pkcm} and Q_{max} during a switch from high to low extracellular Cl. Cells were previously loaded (to steady state) with Cl under high-Cl (80 or 140 mM) extracellular perfusion. Then cells were perfused (starting at -300 s) with 1 mM Cl extracellular medium to unload intracellular Cl. The 0-s mark indicates the beginning of TBT perfusion. Time resolution is 50 s (bin width). During the washout, R_s remained unchanged. The averaged values at the beginning of washout, beginning of TBT perfusion (T0), and the end of washout are 13.2, 12.9, and 13.0 MΩ, respectively. Solid symbols represent control values (1 mM intra/extracellular) before Cl loading. The bars on top show the perfusion strategy. The gray lines are fits to the data; straight line fits were made for the section before TBT, and exponential fits (τ. V_{pkcm}, 35.71 s; Q_{max}, 105.4 s) during TBT perfusion. The control values were used as steady-state end points for the fits.

(Fig. 10). An effect of EtOH on NLC was evident only when the EtOH levels were >1%. In the routine preparation of perfusion solutions that contained TBT, EtOH levels were <0.025%. In the solutions that contained 1 μM TBT, EtOH level was 0.0005%.

Although a low level of EtOH by itself did not cause significant changes in NLC, it is still possible that EtOH may work synergistically with TBT, as has been demonstrated for other ototoxic agents (Loquet et al., 2000). Therefore in a separate set of experiments, TBT was dissolved in the absence of EtOH. In those cases, the actual concentration of TBT is undetermined but is known to be lower than the amount added (in each of three experiments it was <10 μM, <1 μM, and <0.5 μM). The results were similar to those experiments that employed EtOH as solvent for TBT, indicating that the TBT effect is independent of, and not enhanced by, EtOH.

DISCUSSION

In 1991, we showed that the lanthanide, Gd^{+3}, could reversibly block OHC NLC and motility (Santos-Sacchi, 1991); aside from agents that irreversibly damage electromotility (Kalinec and Kachar, 1993), few agents, including salicylate, other lanthanides, and furosemide, have been found to reversibly interfere with lateral membrane motor activity (Dieler et al., 1991; Santos-Sacchi, 2003; Santos-Sacchi et al., 2001; Kakehata and Santos-Sacchi, 1996; Tunstall et al., 1995). After the identification of chloride's preeminent role in promoting prestin activity (Oliver and Fakler, 1999) and the identification of a native pathway for Cl flux within the lateral membrane (Rybalchenko and Santos-Sacchi, 2003c), underlying mechanisms for these blocking agents' actions on OHCs have been revealed. Thus, salicylate, though previously shown to have worked intracellularly in its charged form (Kakehata and Santos-Sacchi, 1996), is now known to interfere with the interaction of Cl and prestin (Oliver et al., 2001); the other agents, in addition to possible direct effects on the motor, may interfere with Cl flux across the lateral membrane (Rybalchenko and Santos-Sacchi, 2003c). These observations have been very helpful in understanding the molecular mechanism responsible for cochlear amplification in mammals (see Santos-Sacchi, 2003).

In this study, we report several new observations that have important consequences for understanding OHC function, and how cochlear amplification may be compromised. First, we show that the ionophore TBT can seriously disrupt chloride homeostasis in the mammalian OHC. Direct measures of chloride flux with the chloride-sensitive dye MQAE, as well as direct measures of chloride-sensitive prestin activity, provide strong evidence for this conclusion. To be sure, TBT was without direct effect on the motor and G_{metL}; the effects were only observed in the presence of a chloride gradient across the OHC membrane, and the

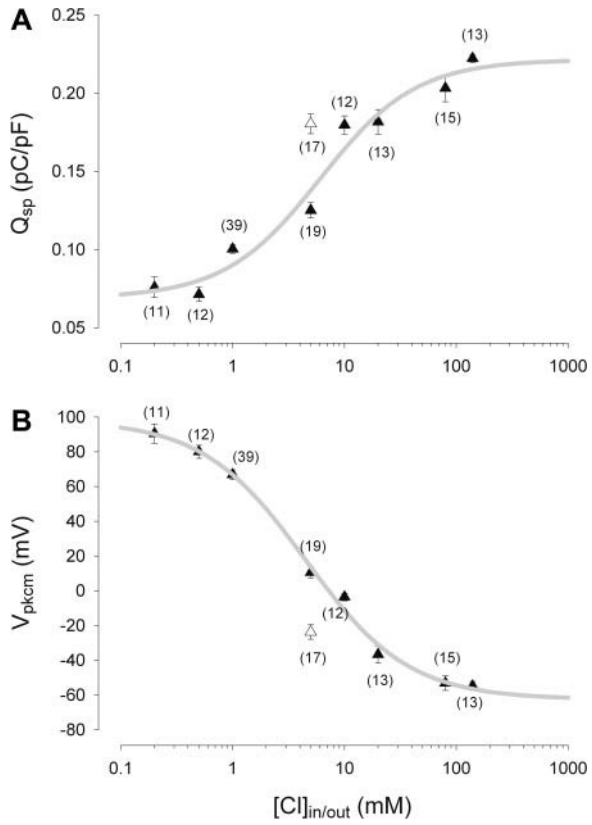

FIGURE 9 Prestin-Cl dose-response relationship. Nonlinear charge density, Q_{sp} and V_{pkcm} as a function of intracellular subplasmalemmal Cl concentrations, are fitted with logistic Hill function (*solid triangles*, malate as substitute anion). Each point represents the average (± SE; *numbers in parentheses*) from pooled recordings with or without TBT, since no statistically significant differences were found. Q_{sp} and V_{pkCm} were measured after pipette washout reached steady state. $K_{1/2}$ for Q_{sp} is 6.06 ± 2.34 mM and slope is 1.02 ± 0.50 (*A*); $K_{1/2}$ for V_{pkcm} data is 4.48 ± 0.77 mM, and slope is 0.94 ± 0.17 (*B*). Open triangles represent values from 5 mM Cl intracellular/extracellular with gluconate as substitute anion. Q_{sp} at steady state is 0.18 as compared to 0.13 in the case of malate substitution, a value that is equivalent to ~16 mM Cl inside with malate substitution.

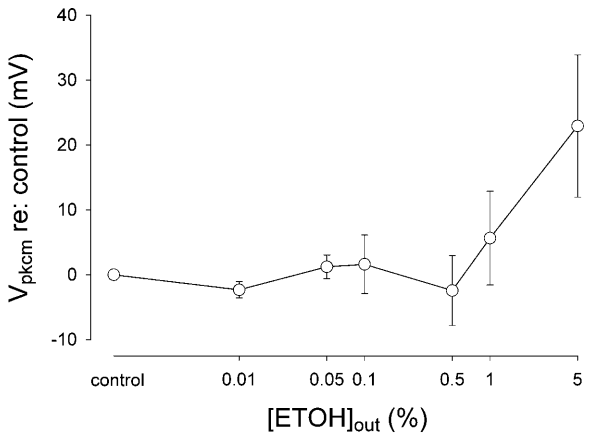

FIGURE 10 Ethyl alcohol shifts the NLC curve to the right at concentrations above 1%. Mean ± SE of V_{pkcm} shift relative to the control are plotted as the function of EtOH concentration. Intracellular Cl is 5 mM in all cases. Q_{max} (not shown) did not change.

magnitude of effects depended on the magnitude of the chloride gradient, with the direction of effects dependent on the direction of the gradient. This behavior was expected from previous work with this agent (Tosteson and Wieth, 1979; Wieth and Tosteson, 1979), and indeed, TBT is used to equilibrate intra- and extracellular chloride for estimation of chloride levels when using chloride-sensitive dyes such as MQAE (Verkman, 1990; Marandi et al., 2002). Second, given TBT's overwhelming effects we were able to compare the efficacy of G_{metL} in permitting chloride flux across the OHC membrane; NLC measures showed that native flux via this conductance is far less efficient than the flux provided by TBT, indicating that G_{metL} contributes to a regulated mechanism for chloride homeostasis within the OHC. Given such an effective agent as TBT, we were able to confirm uncompromised control over intracellular chloride levels and this allowed us, for the first time, to investigate prestin-chloride interactions in the intact OHC. Finally, because of TBT's continued presence within marine environments and its accumulation in the food chain, we identify it as a potential hazard for marine mammals.

The operating range of prestin and lateral membrane Cl flux

Under typical whole-cell voltage-clamp conditions, where 140 mM Cl is perfused intra- and extracellularly, V_{pkcm} resides between −40 and −70 mV (Kakehata and Santos-Sacchi, 1995). This operating position is not fixed, since several fundamental biophysical forces have been shown to shift the NLC function along the voltage axis, i.e., to alter the steady-state energy profile of the lateral membrane motor. These forces include membrane tension (Iwasa, 1993; Gale and Ashmore, 1994; Takahashi and Santos-Sacchi, 2001; Kakehata and Santos-Sacchi, 1995), temperature (Meltzer and Santos-Sacchi, 2001; Santos-Sacchi and Huang, 1998), and voltage (Santos-Sacchi et al., 1998b). Recently, we found that alterations of intracellular Cl concentration can do the same, a decrease in concentration causing a shift in the depolarizing direction (Rybalchenko and Santos-Sacchi, 2003c). Depending on the substitute anion, the position of V_{pkcm} can vary between −180 and greater than +100 mV.

In the absence of TBT, chloride can permeate the lateral membrane through the stretch-activated conductance, G_{metL}. Under whole-cell voltage clamp, however, the effectiveness of this native conductance in modulating intracellular levels of chloride, in the face of changes in the extracellular Cl driving force depends on the pipette washout rate. Thus, after achieving steady-state conditions in the presence of 1 mM Cl within the patch pipette and extracellularly, an increase in extracellular Cl levels leads to a hyperpolarizing shift in V_{pkcm}, demonstrating that intracellular Cl increases as a result

of the imposed chemical driving force. However, the shift in V_{pkcm} does not recover to initial levels, and indicates that G_{metL}-mediated Cl flux is not sufficient to counteract the continuous washout of Cl by intracellular pipette perfusion. Clearly, if G_{metL} were to provide no barrier to the passage of Cl, the OHC could not use this ion as a modulator of prestin. The limiting nature of this native conductance was confirmed by treatment with TBT, which augmented Cl flux and returned V_{pkcm} further back toward initial conditions. Washout of cellular constituents via pipette is an efficient process, with replacements typically occurring within a few minutes (Pusch and Neher, 1988). It is surprising, therefore, that TBT can work so efficiently against pipette washout of Cl, and it may be possible that the restricted nature of the lateral subplasmalemmal space (LSpS) aids this process (see discussion in Rybalchenko and Santos-Sacchi, 2003c). Of course, in the intact OHC, G_{metL} will not have to struggle against such a powerful buffering mechanism as artificial pipette washout.

In our experiments on efflux of Cl from the OHC, we found a barrier to the complete washout of Cl from the LSpS, after Cl loading (Fig. 8). Whereas the influx of Cl during perfusion of high extracellular Cl competes with pipette washout, the efflux of Cl during perfusion of low extracellular Cl levels should be augmented by pipette washout. Despite this, TBT was required to fully allow Cl efflux, and may indicate some type of rectification of the native conductance, G_{metL}. However, our direct electrophysiological evaluation of G_{metL} showed no rectification near our holding potential of 0 mV (Rybalchenko and Santos-Sacchi, 2003c). Instead, we suspect that the conductance magnitude of G_{metL} may have changed during the shifts between low and high chloride. Perhaps lateral membrane tension was altered, thus altering the activation state of the pathway. Alternatively, exposure of G_{metL} to low Cl levels may have altered its activity, as has been found to occur in K channels (Loboda et al., 2001; Melishchuk et al., 1998).

Anion effects on motor charge movement–Q_{max}

In vivo, the flux of Cl across the lateral membrane through G_{metL} will be governed by membrane potential, membrane tension, and chloride's chemical driving force (Rybalchenko and Santos-Sacchi, 2003c). We have estimated intracellular Cl levels to be <9 mM at the normal in vivo resting potential (see Rybalchenko and Santos-Sacchi, 2003c), which places the cell in a maximally responsive region of the Q_{max}-Cl curve (Fig. 9). Interestingly, we again obtain a Q_{max}-Cl relationship in intact OHCs that differs substantially from that obtained by Oliver et al. in membrane patches (Oliver et al., 2001). Previously, we obtained an estimate of the Q_{max}-Cl function from OHCs by utilizing the conductive power of G_{metL} to control Cl on either side of the lateral membrane (Rybalchenko and Santos-Sacchi, 2003c). In those experiments, Cl concentration ranges from zero to 140 mM were evaluated, but we found that peak NLC could not be decreased below $\sim$0.4 of control levels. This contrasted with the results of Oliver et al. (2001), where even 1-mM concentrations of Cl reduced Q_{max} to 0.15 of control values. In this set of experiments, to ensure against noise and drift caused by zero Cl levels, we did not lower Cl below 0.2 mM and employed TBT to ensure robust control of Cl concentration on either side of the lateral membrane. Nevertheless, we were unable to reduce motor charge movement (Q_{max}) to those levels found by Oliver et al. (2001); our Q_{max} levels at 0.2 mM Cl remain at 0.36 (1.15 $\pm$ 0.09 pC; $n = 11$) of saturated values (Fig. 9). Thus, $\sim$36% of motor charge movement is insensitive to Cl, and reinforces our prior suggestions that Cl does not simply serve as prestin's extrinsic voltage sensor (Rybalchenko and Santos-Sacchi, 2003a,c). For that fraction of charge that is regulated by Cl, we find a $K_{1/2}$ (6.06 mM) and slope (1.02) that closely correspond to those measures of Oliver et al (2001). It should be noted that the other physiological anion that affects prestin is bicarbonate, whose $K_{1/2}$ is 44 mM (Oliver et al., 2001), and which, under our intracellular and extracellular perfusion conditions, cannot reasonably account for the Cl-insensitive component of Q_{max}.

How is it that Cl is only partially responsible for charge movement of the OHC motor? It may be that prestin presents characteristics substantially similar to those of other transporters capable of charge movement under appropriate conditions, as evidenced by presteady-state currents (which are equivalent to an NLC) (Sacher et al., 2002; Hazama et al., 1997). Thus, in the absence of substrate, transporters such as mGAT3 and SGLT1 produce voltage-dependent displacement currents which may dependent upon ion binding/dissociation or intrinsic conformational change. Interestingly, the GABA transporter's charge-movement dependence on Cl is not absolute (Sacher et al., 2002). We reason that the OHC motor likely possesses intrinsic charge movement due to conformational change, induced either by voltage or tension. Notably, those displacement currents displayed by transporters are typically abolished by saturating concentrations of appropriate substrate. Are we unaware of a natural substrate for prestin (SLC26a5), which normally works to dilute OHC NLC and motor activity?

Cl effect on OHC mechanics

NLC and electromotility are inextricably related; namely, shifts in V_{pkcm} along the voltage axis are mirrored in the mechanical activity of the OHC (Wu and Santos-Sacchi, 1998; Kakehata and Santos-Sacchi, 1995, 1996; Santos-Sacchi, 1991). Thus, OHC length is expected to change as V_{pkcm} shifts during intracellular chloride modulation simply because the drive to prestin is governed by the position of its Q-V or NLC function along the voltage axis. At a fixed holding voltage, a hyperpolarizing shift in V_{pkcm} will be sensed as a depolarizing stimulus by the lateral membrane motors, causing the cell to contract, as we illustrated (Fig. 7). Viewed as a population of motors, the percentage of motors

occupying the contracted state will increase; or for a given motor, the probability that that motor will reside in the contracted state will increase. A similar effect will also occur when Cl is modulated by pipette perfusion. In addition to direct effects of Cl on the motor, another possible mechanism could contribute to changes in cell length within the timescale that we worked under whole-cell voltage clamp, namely, water uptake after Cl influx. The expected magnitude of the voltage-induced contraction is easily calculated based on known OHC length-V_m functions. The contraction due to water movement can be quite large, and may overwhelm that induced by a perceived change in voltage. The cell in Fig. 7 shows a contraction of 4.4 μm. The average change in V_{pkcm} during a change from 1 mM extracellular solution to a saturating Cl solution (namely, 80 mM or above in 1 μM TBT's presence; Fig. 8) is $\sim$15 mV. Given the largest measured mechanical response of 30 nm/mV (Santos-Sacchi and Dilger, 1988), we calculate that a half-micrometer contraction must occur. So in addition to an expected half-micrometer voltage-induced response, we likely have an additional 4 μm response due to water movements.

Based on these results, it is imperative that the consequences of chloride-induced shifts in V_{pkcm} and water movements be considered when evaluating effects of Cl manipulations on OHC mechanical characteristics. For example, OHC stiffness, which has been shown to be voltage-dependent in a manner that mimics electromotility (He and Dallos, 2000), will necessarily change when Cl-induced changes in V_{pkcm} occur, even if motor charge movement remains unaltered. Thus, it is not at all clear whether changes in voltage drive to the motor or changes in motor sensitivity underlie the effects of Cl manipulations on OHC stiffness (He et al., 2003). Indeed, controlling for these shifts is especially important when using anion substitutes such as pentane sulfonate (He and Dallos, 2000), which can cause V_{pkcm} to shift to very negative potentials (Rybalchenko and Santos-Sacchi, 2003b,c). Such a shift would cause the OHC to respond as it would to a depolarizing stimulus, namely, with a decrease in the cell's stiffness. In such a case, evaluations made across a full range of voltages are required for proper assessments of Cl's role.

The ototoxic effect of organotins

In this study we have shown that TBT functions as an ionophore that can bypass the native Cl pathway, G_{metL}. In effect, prestin is no longer subject to Cl modulation, and thus cochlear amplification will likely suffer. Whereas the other organotins, TET and TMT, have been shown to reduce auditory sensitivity in mammals (Clerici et al., 1991; Fechter et al., 1986, 1992; Liu and Fechter, 1995), their major action is considered to be at the inner hair cell/spiral ganglion cell level, and involve disruption of Ca homeostasis.

The ineffectiveness of TBT in the absence of a chloride gradient between intra and extracellular spaces indicates that TBT does not affect the motor directly, and that any other possible intermediary effect on the motor resulting from TBT treatment is absent within our experimental timeframe; this precludes possible Ca effects as well. Additionally, the observed rapid effects of TBT (within seconds) differs from the slow (>30 min) cell shortening action of other trialkyltins on OHCs (Clerici et al., 1991; Fechter et al., 1986, 1992; Liu and Fechter, 1995). Indeed, Frolenkov et al (2000) showed that intracellular Ca increases caused by ionomycin or ACh, with or without perforated patch, produced no changes in OHC NLC. They did find, however, that phosphorylating and dephosphorylating agents, after 30–60 min incubation, resulted in V_{pkcm} shifts but had no effect on Q_{max}. To be sure, these results cannot be reconciled with our data on TBT effects, which show 1), a requirement for a Cl gradient; 2), simultaneous effects on both V_{pkcm} and Q_{max}; 3), a dependence on magnitude and direction of the chloride gradient; that is, relative to initial conditions, the degree of V_{pkcm} shift and magnitude of Q_{max} depend on the magnitude of the Cl gradient, and the direction of V_{pkcm} shift depends on the direction of the Cl gradient; 4), rapid onset, within seconds; and 5), insensitivity to intracellular Ca buffer (10 mM EGTA). These observations indicate that the effects of TBT on the OHC result from Cl effects and not those of Ca. Interestingly, though, our results that organotins foster chloride flux across the OHC membrane may partially underlie their observed ability to shorten OHCs (Clerici et al., 1993), since, as we discussed above, binding of chloride ions to prestin increases the probability of the motor's residence in the contracted state.

Finally, we believe that the marine pollutant TBT poses a serious threat to marine mammals in particular, since they share with us the benefits of cochlear amplification. There are a growing number of studies linking TBT to untoward effects on mammalian cellular processes. For example, Akaike's group (Kishimoto et al., 2001) has found that environmentally relevant concentrations (30–100 nM) influence GABAergic neurotransmission, and suggested that some marine food sources which can accumulate TBT at levels of 100 nM or more pose a human health risk. Marine mammals likewise are exposed to this risk, perhaps more so. It will be important to assess the impact of TBT exposure on marine mammal communication.

We thank Dr. John Geibel (Yale Dept. of Surgery) for help with the MQAE dye experiments and the use of his equipment. We also thank Margaret Mazzucco for technical help.

This research was supported by National Institutes of Health National Institute on Deafness and Other Communication Disorders grant DC000273 to J.S.S.

REFERENCES

Ashmore, J. F. 1987. A fast motile response in guinea-pig outer hair cells: the cellular basis of the cochlear amplifier. *J. Physiol.* 388:323–347.

Belyantseva, I. A., H. J. Adler, R. Curi, G. I. Frolenkov, and B. Kachar. 2000. Expression and localization of prestin and the sugar transporter

GLUT-5 during development of electromotility in cochlear outer hair cells. *J. Neurosci.* 20:RC116.

Brownell, W. E., C. R. Bader, D. Bertrand, and Y. de Ribaupierre. 1985. Evoked mechanical responses of isolated cochlear outer hair cells. *Science.* 227:194–196.

Clerici, W. J., M. E. Chertoff, W. E. Brownell, and L. D. Fechter. 1993. In vitro organotin administration alters guinea pig cochlear outer hair cell shape and viability. *Toxicol. Appl. Pharmacol.* 120:193–202.

Clerici, W. J., B. Ross, Jr., and L. D. Fechter. 1991. Acute ototoxicity of trialkyltins in the guinea pig. *Toxicol. Appl. Pharmacol.* 109:547–556.

Dallos, P., J. Santos-Sacchi, and A. Flock. 1982. Intracellular recordings from cochlear outer hair cells. *Science.* 218:582–584.

Dieler, R., W. E. Shehata-Dieler, and W. E. Brownell. 1991. Concomitant salicylate-induced alterations of outer hair cell subsurface cisternae and electromotility. *J. Neurocytol.* 20:637–653.

Fechter, L. D., W. J. Clerici, L. Yao, and V. Hoeffding. 1992. Rapid disruption of cochlear function and structure by trimethyltin in the guinea pig. *Hear. Res.* 58:166–174.

Fechter, L. D., J. S. Young, and A. L. Nuttall. 1986. Trimethyltin ototoxicity: evidence for a cochlear site of injury. *Hear. Res.* 23:275–282.

Frolenkov, G. I., F. Mammano, I. A. Belyantseva, D. Coling, and B. Kachar. 2000. Two distinct Ca(2+)-dependent signaling pathways regulate the motor output of cochlear outer hair cells. *J. Neurosci.* 20:5940–5948.

Gale, J. E., and J. F. Ashmore. 1994. Charge displacement induced by rapid stretch in the basolateral membrane of the guinea-pig outer hair cell. *Proc. R. Soc. Lond. B. Biol. Sci.* 255:243–249.

Gitter, A. H., H. P. Zenner, and E. Fromter. 1986. Membrane potential and ion channels in isolated outer hair cells of guinea pig cochlea. *ORL J. Otorhinolaryngol. Relat. Spec.* 48:68–75.

Hazama, A., D. D. Loo, and E. M. Wright. 1997. Presteady-state currents of the rabbit Na+/glucose cotransporter (SGLT1). *J. Membr. Biol.* 155: 175–186.

He, D. Z., and P. Dallos. 2000. Properties of voltage-dependent somatic stiffness of cochlear outer hair cells. *J. Assoc. Res. Otolaryngol.* 1:64–81.

He, D. Z., S. Jia, and P. Dallos. 2003. Prestin and the dynamic stiffness of cochlear outer hair cells. *J. Neurosci.* 23:9089–9096.

Huang, G., and J. Santos-Sacchi. 2003. Motility voltage sensor of the outer hair cell resides within the lateral plasma membrane. *Proc. Natl. Acad. Sci. USA.* 91:12268–12275.

Iwasa, K. H. 1993. Effect of stress on the membrane capacitance of the auditory outer hair cell. *Biophys. J.* 65:492–498.

Kakehata, S., and J. Santos-Sacchi. 1995. Membrane tension directly shifts voltage dependence of outer hair cell motility and associated gating charge. *Biophys. J.* 68:2190–2197.

Kakehata, S., and J. Santos-Sacchi. 1996. Effects of salicylate and lanthanides on outer hair cell motility and associated gating charge. *J. Neurosci.* 16:4881–4889.

Kalinec, F., and B. Kachar. 1993. Inhibition of outer hair cell electromotility by sulfhydryl specific reagents. *Neurosci. Lett.* 157:231–234.

Kawasaki, E., N. Hattori, E. Miyamoto, T. Yamashita, and C. Inagaki. 1999. Single-cell RT-PCR demonstrates expression of voltage-dependent chloride channels (ClC-1, ClC-2 and ClC-3) in outer hair cells of rat cochlea. *Brain Res.* 838:166–170.

Kishimoto, K., S. I. Matsuo, Y. Kanemoto, H. Ishibashi, Y. Oyama, and N. Akaike. 2001. Nanomolar concentrations of tri-n-butyltin facilitate gamma-aminobutyric acidergic synaptic transmission in rat hypothalamic neurons. *J. Pharmacol. Exp. Ther.* 299:171–177.

Liberman, M. C., J. Gao, D. Z. He, X. Wu, S. Jia, and J. Zuo. 2002. Prestin is required for electromotility of the outer hair cell and for the cochlear amplifier. *Nature.* 419:300–304.

Liu, Y., and L. D. Fechter. 1995. Trimethyltin disrupts loudness recruitment and auditory threshold sensitivity in guinea pigs. *Neurotoxicol. Teratol.* 17:281–287.

Loboda, A., A. Melishchuk, and C. Armstrong. 2001. Dilated and defunct K channels in the absence of K+. *Biophys. J.* 80:2704–2714.

Loquet, G., P. Campo, R. Lataye, B. Cossec, and P. Bonnet. 2000. Combined effects of exposure to styrene and ethanol on the auditory function in the rat. *Hear. Res.* 148:173–180.

Marandi, N., A. Konnerth, and O. Garaschuk. 2002. Two-photon chloride imaging in neurons of brain slices. *Pflugers Arch.* 445:357–365.

Melishchuk, A., A. Loboda, and C. M. Armstrong. 1998. Loss of shaker K channel conductance in 0 K+ solutions: role of the voltage sensor. *Biophys. J.* 75:1828–1835.

Meltzer, J., and J. Santos-Sacchi. 2001. Temperature dependence of nonlinear capacitance in human embryonic kidney cells transfected with prestin, the outer hair cell motor protein. *Neurosci. Lett.* 313:141–144.

Motais, R., J. L. Cousin, and F. Sola. 1977. The chloride transport induced by triaklyl-tin compound across erythrocyte membrane. *Biochim. Biophys. Acta.* 467:357–363.

Oliver, D., and B. Fakler. 1999. Expression density and functional characteristics of the outer hair cell motor protein are regulated during postnatal development in rat. *J. Physiol. (Lond).* 519:791–800 In press.

Oliver, D., D. Z. He, N. Klocker, J. Ludwig, U. Schulte, S. Waldegger, J. P. Ruppersberg, P. Dallos, and B. Fakler. 2001. Intracellular anions as the voltage sensor of prestin, the outer hair cell motor protein. *Science.* 292:2340–2343.

Pusch, M., and E. Neher. 1988. Rates of diffusional exchange between small cells and a measuring patch pipette. *Pflugers Arch.* 411:204–211.

Rybalchenko, V., and J. Santos-Sacchi. 2003a. Allosteric modulation of the outer hair cell motor protein prestin by chloride. *In* Biophysics of the Cochlea: From Molecules to Models. A. Gummer, editor. World Scientific Publishing, Singapore. 116–126.

Rybalchenko, V., and J. Santos-Sacchi. 2003b. Modulation of the outer hair cell motor by sulfonate-containing anions. *Assoc. Res. Otolaryngol. Abs.* 209.

Rybalchenko, V., and J. Santos-Sacchi. 2003c. Cl- flux through a non-selective, stretch-sensitive conductance influences the outer hair cell motor of the guinea-pig. *J. Physiol.* 547:873–891.

Sacher, A., N. Nelson, J. T. Ogi, E. M. Wright, D. D. Loo, and S. Eskandari. 2002. Presteady-state and steady-state kinetics and turnover rate of the mouse gamma-aminobutyric acid transporter (mGAT3). *J. Membr. Biol.* 190:57–73.

Santos-Sacchi, J. 1991. Reversible inhibition of voltage-dependent outer hair cell motility and capacitance. *J. Neurosci.* 11:3096–3110.

Santos-Sacchi, J. 2003. New tunes from Corti's organ: the outer hair cell boogie rules! *Curr. Opin. Neurobiol.* In press.

Santos-Sacchi, J. 2004. Determination of cell capacitance using the exact empirical solution of partial differential Y/partial differential C_m and its phase angle. *Biophys. J.* 87:714–727.

Santos-Sacchi, J., and J. P. Dilger. 1988. Whole cell currents and mechanical responses of isolated outer hair cells. *Hear. Res.* 35:143–150.

Santos-Sacchi, J., and G. Huang. 1998. Temperature dependence of outer hair cell nonlinear capacitance. *Hear. Res.* 116:99–106.

Santos-Sacchi, J., S. Kakehata, T. Kikuchi, Y. Katori, and T. Takasaka. 1998a. Density of motility-related charge in the outer hair cell of the guinea pig is inversely related to best frequency. *Neurosci. Lett.* 256:155–158.

Santos-Sacchi, J., S. Kakehata, and S. Takahashi. 1998b. Effects of membrane potential on the voltage dependence of motility-related charge in outer hair cells of the guinea-pig. *J. Physiol (Lond).* 510:225–235.

Santos-Sacchi, J., and E. Navarrete. 2002. Voltage-dependent changes in specific membrane capacitance caused by prestin, the outer hair cell lateral membrane motor. *Pflugers Arch.* 444:99–106.

Santos-Sacchi, J., M. Wu, and S. Kakehata. 2001. Furosemide alters nonlinear capacitance in isolated outer hair cells. *Hear. Res.* 159:69–73.

Selwyn, M. J., A. P. Dawson, M. Stockdale, and N. Gains. 1970. Chloride-hydroxide exchange across mitochondrial, erythrocyte and artificial

lipid membranes mediated by trialkyl- and triphenyltin compounds. *Eur. J. Biochem.* 14:120–126.

Takahashi, S., and J. Santos-Sacchi. 2001. Non-uniform mapping of stress-induced, motility-related charge movement in the outer hair cell plasma membrane. *Pflugers Arch.* 441:506–513.

Tosteson, M. T., and J. O. Wieth. 1979. Tributyltin-mediated exchange diffusion of halides in lipid bilayers. *J. Gen. Physiol.* 73:789–800.

Tunstall, M. J., J. E. Gale, and J. F. Ashmore. 1995. Action of salicylate on membrane capacitance of outer hair cells from the guinea-pig cochlea. *J. Physiol.* 485:739–752.

U.S. Environmental Protection Agency. 2004. Notice of availability of final aquatic life criteria document for tributyltin (TBT). *Fed. Regist.* 69:342–343 (USA).

Verkman, A. S. 1990. Development and biological applications of chloride-sensitive fluorescent indicators. *Am. J. Physiol.* 259:C375–C388.

Wieth, J. O., and M. T. Tosteson. 1979. Organotin-mediated exchange diffusion of anions in human red cells. *J. Gen. Physiol.* 73:765–788.

Wu, M., and J. Santos-Sacchi. 1998. Effects of lipophilic ions on outer hair cell membrane capacitance and motility. *J. Membr. Biol.* 166:111–118.

Zheng, J., W. Shen, D. Z. He, K. B. Long, L. D. Madison, and P. Dallos. 2000. Prestin is the motor protein of cochlear outer hair cells. *Nature.* 405:149–155.